Covid-19 Detection Based on Chest X-Ray Images Using DCT Compression and NN

Fatma Taher
College of Technological Innovation
Zayed University
Dubai, UAE
Fatma.Taher@zu.ac.ae

Reem T Haweel
Computers and Information sciences
Ain Shams University
Cairo, Egypt
Reem.T.Haweel@cis.asu.edu.eg

Usama Mohammad Hassan Al Bastaki
Radiology Department
Rashid Hospital
Dubai, UAE
UMALBastaki@dha.gov.ae

Eman Abdelwahed
Radiology Department
Rashid Hospital
Dubai, UAE
emabdou@dha.gov.ae

Tariq Rehman
Radiology Department
Rashid Hospital
Dubai, UAE
tariqfr@dha.gov.ae

Tarek I Haweel
Electrical Engineering Department
Assiut University
Assiut, Egypt
t.haweel@aun.edu.eg

2022 IEEE International Conference on Imaging Systems and Techniques (IST) | 978-1-6654-8102-1/22/$31.00 ©2022 IEEE | DOI: 10.1109/IST55454.2022.9827673

***Abstract*— Covid-19 is a highly contagious virus spreading all over the world. It is caused by SARS-CoV-2. virus. Some of the most common symptoms are fever, cough, sore throat, tiredness, and loss of smell or taste. There are two types of tests for COVID-19: the PCR test and the antigen test. Automatic detection of Covid-19 from publicly available resources is essential. This paper employs the commonly available chest X-ray (CXR) images in the classification of Covid-19, normal and viral pneumonia cases. The proposed method divides the CXR images into subblocks and computes the Discrete Cosine Transform (DCT) for every subblock. The DCT energy compaction capability is employed to produce a compressed version for each CXR image. Few spectral DCT components are incorporated as features for each image. The compressed images are scanned by average pooling windows to reduce the dimension of the final feature vectors. A multilayer artificial neural network is employed in the 3-set classification. The proposed method achieved an average accuracy of 95 %. While the proposed method achieves comparable accuracy relative to recent state-of-the-art techniques, its computational burden and implementation time is much less.**

Keywords*— *COVID-19 detection, pneumonia, Chest X-ray, discrete cosine transform, lossy compression, medical image classification, neural networks.

I. Introduction

The coronavirus of 2019, widely termed as COVID-19, targets the respiratory system and the lungs causing severe levels of pneumonia. Early detection of COVID-19 is important to limit the expansion of such pandemic Polymerase chain reaction (PCR) is the most widely used technique for detecting COVID-19. However, PCR may not be available in underdeveloped regions and its sensitivity is low [1]. Moreover, PCR is time-consuming and exhibits high false-negative levels [2]. On the other hand, Chest radiography, especially CXR, is worldwide performed in diagnosis and may be employed to track the pathological signature of COVID-19 on the CXR of suspected patients [3],[4]. Unfortunately, the CXR abnormalities caused by COVID-19 are similar to those of viral pneumonia [5],[6]. Automation is required to accurately detect and differentiate COVID-19 and pneumonia.

Artificial intelligence, such as machine and deep learning, has been employed to achieve such automation based on CXR [7]. A deep learning approach to detect COVID-19 and viral pneumonia was achieved in [8] implementing ResNet-101 with high accuracy. ResNet-50 architecture along with the SVM classifier also produced good accuracy [9]. Makris et al [10]. employed several convolutional neural networks (CNN) models and compared their performances in classifying COVID-19, pneumonia, and normal images [10]. Asif et al. [11] trained InceptionV3 using transfer learning techniques to distinguish COVID-19 from viral pneumonia and normal CXR and obtained a high accuracy. Das et al. [12] have developed an interesting model using ensemble average learning employing three pre-trained CNN networks; DenseNet201, Resnet50V2, and InceptionV3 achieved high accuracy and sensitivity. Ridhi et al. [13] classified COVID-19, pneumonia, and normal CXR employing stacked of DenseNet and GoogleNet. Gupta et al. [14] implemented a CNN network termed InstaCovNet-19 integrating several deep networks and achieved high accuracy both in binary (COVID-19 vs non-COVID-19) and in 3-class (COVID-19, pneumonia, normal) classifications. Another CNN network was proposed in [15] which achieved high accuracy for binary, 3-class, and 4-class classifications. Canayaz et al. [16] proposed a diagnosis of COVID-19 using deep neural networks and meta-heuristic-based feature selection and achieved very high accuracy. Khuzani et al. [17] employed features extracted using the spatial domain (GLCM, GLDM, Texture), spectral-domain (FFT), and spacio-spectral-domain (Wavelet) transforms fed to a feedforward neural network for a 3-class classification; COVID-19, pneumonia, and normal [17]. It is shown in [17] that features associated with the spectral domain have better prediction power than the other groups (spatial and spacio-spectral) regarding Covid-19 prediction from CXR images.

This work presents a simple but efficient method for 3-class classification; COVID-19, normal, and pneumonia. The proposed method employs the energy compaction property of the DCT for a compressed spectral domain feature extraction. The rest of the paper is organized as follows. Section II summarizes the essential properties of the DCT. The proposed technique is illustrated in Section III. A discussion is given in Section IV to elaborate on the main advantages of the proposed technique over the present state-of-the-art methods. Finally, Section V concludes the work.

II. Discrete Cosine Transform

The DCT incorporates real sinusoids and has many interesting features. In addition to its orthogonal structure, the

978-1-6654-8102-1/22/$31.00 ©2022 IEEE

DCT has excellent energy concentration properties. Only 10% of the DCT spectral components contain about 90% of the total signal power [18]. Consequently, the DCT is the core of multimedia image and video compression techniques such as Joint Photographic Experts Group (JPEG) and Moving Picture Experts Group (MPEG) compression standards [19]. Moreover, the DCT has good decorrelating properties and may be employed to reduce the inherent high correlation that exists between the rows and columns of images [20]. The elements of matrix T of one-dimensional DCT in the case of N-element input vectors can be defined as follows:

$$T_{kn} = \alpha(k)\cos\left(\frac{\pi}{N}k\left[n+\frac{1}{2}\right]\right) \quad (1)$$

For $k, n = 0,1,\ldots,N-1$, with $\alpha(k) = \sqrt{1/N}$ for $k = 0$ and $\alpha(k) = \sqrt{2/N}$ otherwise.

Another advantage of DCT is its two-dimensional separability. If X is an input image, then its representation Y in the transform domain of two-dimensional DCT can be calculated as

$$Y = TXT^t \quad (2)$$

Modern image applications partition input images into 8 ×8-pixel blocks. Consequently, 8×8 DCT has been given special consideration to provide for approximations that are computationally simple. Since the pioneering work by Haweel et al.[18] that explored a DCT approximation requiring only 24 additions, many other approximations have been introduced in the literature. A comparative study for all effective approximations has been analyzed in [20].

III. Proposed Technique

A. Dataset

The employed data set contained the CXR images of COVID-19 positive cases, normal and viral pneumonia cases. These CXR images were produced at Rashid hospital radiology department in the United Arab Emirates. Balanced sets were selected where each of the three sets contains 600 CXR images. Images are in JPEG format having a dimension of 1024x1024 pixels.

B. Feature Extraction

All images are resized to 256x256 gray scale and every image is scanned by an 8x8 mask. The two-dimensional DCT are computed for each masked block using (2). Out of the 64 spectral components, only the highest 8 transform pixels (top left) are retained while all other transformed pixels are discarded. That is, all images have been compressed by a factor of 8. To illustrate the quality of the compressed CXR images, the discarded pixels are zeroed and the masked blocks are transformed back to the spatial domain using

$$\hat{X} = T^t Y T \quad (3)$$

Figure 1 shows the original and the compressed reconstructed images for a normal case. The subjective good quality of the compressed image is clear. The percentage error energy norm (PEEN) has been computed as an objective measure for the degradation caused by compression. The PEEN is defined as [18]

$$PEEN = \sqrt{\frac{\sum_{m=0}^{M-1}\sum_{n=0}^{M-1}(I(m,n)-IR(m,n))^2}{\sum_{m=0}^{M-1}\sum_{n=0}^{M-1}I^2(m,n)}}\times 100 \quad (4)$$

Where $I(m,n)$ is the original CXR image and $IR(m,n)$ is the reconstructed (compressed) image.

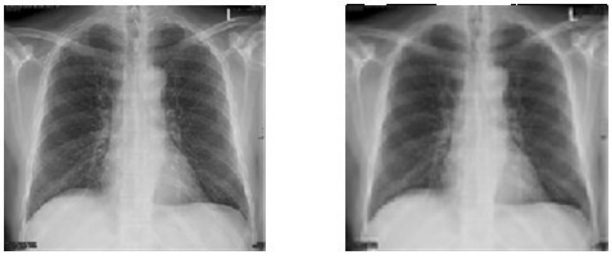

Figure 1. Original and compressed Normal CXR image

Table I illustrates the PEEN for the three cases which indicates that they are all low and almost equal. Since this slight degradation due to compression is almost the same for the three sets, the effect of compression on the classification stage is negligible.

TABLE I. PEEN For Compressed CXR Images

	Normal	***Covid-19***	***Pneumonia***
PEEN	3.5845	3.5033	3.5066

The retained highest 8 transformed pixels for each 8x8 block is concatenated to form one 8-pixels raw. So that, the compressed image size is now 32x256. A pooling averaging window mask of 4x4 is performed for every compressed image twice. At the first run, the averaged resulting image size is 8x64 and after the second run the size is 2x16. The final averaged image is flattened to produce a 32-feature vector for each CXR image in each class. Figure 2 illustrates the feature extraction methodology.

C. Classification

A feedforward neural network is employed to classify the three sets as shown in Figure 3. The input layer is 32 neurons corresponding to the 32-feature vectors. Two hidden layers with 50 and 20 neurons respectively are used. The number of neurons in the hidden layers were optimized for best performance. The output layer has 3 neurons corresponding to the three classified sets. The upper output neuron is on (has a value of 1) if the 32-feature vector corresponds to the normal set, the middle neuron is on for Covid-19 feature vector and finally the last output neuron is on for pneumonia feature vector as shown in (5) where O is the output (target) matrix.

$$O = [N \quad C \quad P] = \begin{bmatrix} 1 & 0 & 0 \\ 0 & 1 & 0 \\ 0 & 0 & 1 \end{bmatrix} \tag{5}$$

The transfer functions for the neurons connecting the second hidden layer to the output neurons are log-sigmoid since the swing of the outputs are between zero and one.

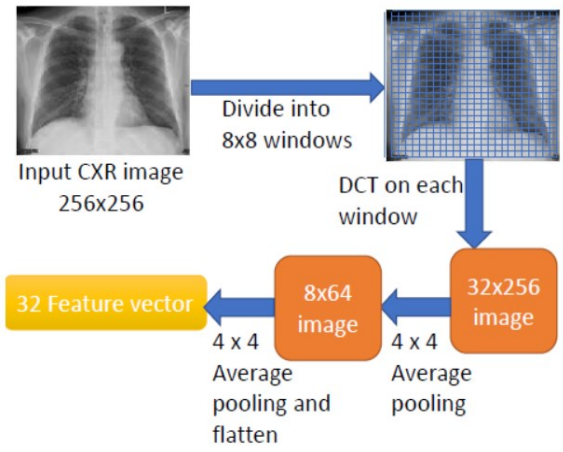

Figure 2. Feature extraction steps

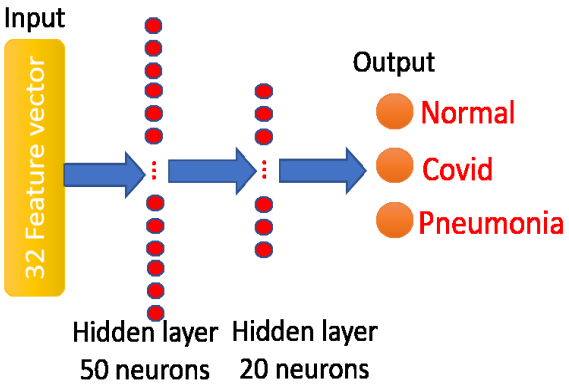

Figure 3. Employed multilayer neural network for classification

The Levenberg-Marquardt algorithm has been employed for updating the suggested neural network. Like the quasi-Newton methods, the Levenberg-Marquardt algorithm is designed to approach second-order training speed without having to compute the Hessian matrix [21]. The Hessian matrix, H, can be approximated as

$$H = J^t J \tag{6}$$

and the gradient can be estimated as

$$g = J^t e \tag{7}$$

where $\boldsymbol{J}$ is the Jacobian matrix that contains first derivatives of the network errors with respect to the weights and biases, and $\boldsymbol{e}$ is a vector of network errors. The Levenberg-Marquardt algorithm uses this approximation to the Hessian matrix in the following Newton-like update to minimize the mean squared error (MSE)

$$X_{k+1} = X_k - [J^t J + \mu I]^{-1} J^t e \tag{8}$$

Where μ is an adaptation variable. The Levenberg-Marquardt is fast and more accurate near an error minimum where μ is highly reduced near the minimum [22]. The number of inputs CXR images employed in the training session is 500 images from each class (total of 15000 images). The MSE learning curve is shown in Figure 4 where the very fast convergence near the minimum MSE is clear. The training algorithm reached a MSE of about -90 dB in 88 epochs only. Figure 5 shows the variation of μ during the training phase. The start value of μ is 1e-3 and the final value is 1e-15. It is also noted that μ has been highly reduced near the minimum MSE as expected. Validation tests have been performed to ensure that the employed neural network did not overfit or underfit the input data (features derived from the three-set CXR images).

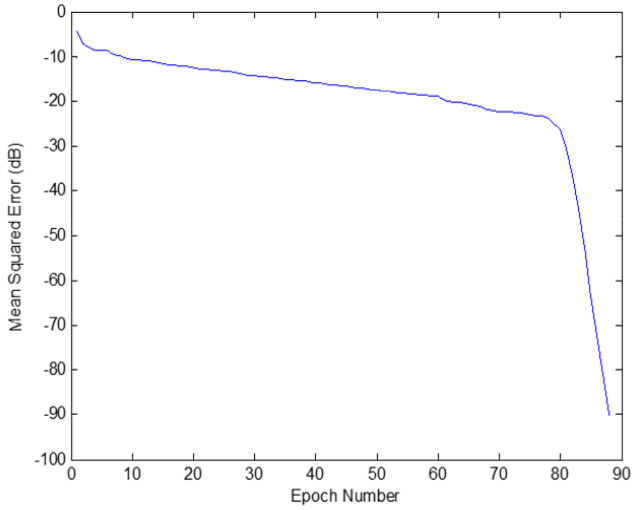

Figure 4. Learning curve for the classification neural network

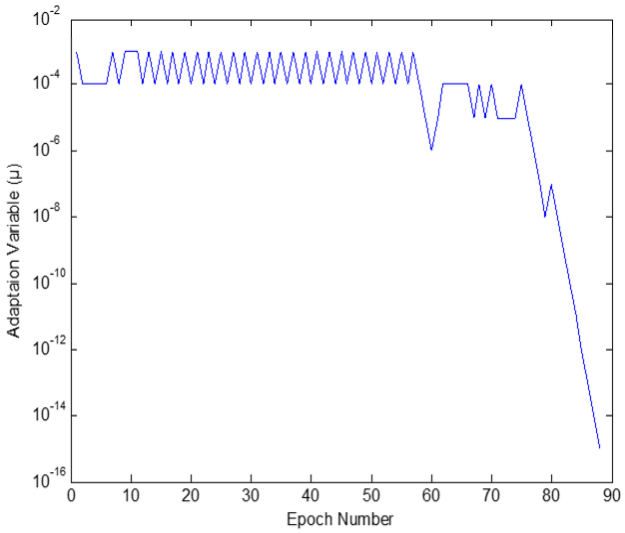

Figure 5. Variation of μ during the training phase

The convergent neural network has been tested using 100 images from each class (total of 300 images). As an indication to the test phase of the proposed technique, five output vectors corresponding to true positive COVID-19 CXR cases are listed in Table II which shows the almost one and zeros at the expected positions.

TABLE II. OUTPUTS FOR TRUE POSITIVE COVID-19 CXR CASES

4.9923e-08	8.2066e-11	2.7338e-08	1.0418e-12	8.5371e-11
1.0000e+00	1.0000e+00	1.0000e+00	1.0000e+00	1.0000e+00
1.0093e-07	3.8957e-08	7.3039e-07	5.1293e-10	1.9430e-11

D. Performance

The confusion matrix is commonly used to evaluate the classification performance of a network. Table III illustrates the elements of the confusion matrix

TABLE III. CONFUSION MATRIX

	Predicted Positive	***Predicted Negative***
Actual Positive	True Positive (TP)	False Negative (FN)
Actual Negative	False Positive (FP)	True Negative (TN)

The following metrics are commonly employed; Accuracy, Precision, Recall (Sensitivity), and F1-score, e.g. [7], [23]. In the case of balanced data set multiclass classification, these metrics are defined as follows [24].

$$Accuracy = \frac{\sum_{i=1}^{M} \frac{TP_i+TN_i}{TP_i+FN_i+FP_i+TN_i}}{M} \quad (9)$$

$$Precision = \frac{\sum_{i=1}^{M} \frac{TP_i}{TP_i+FP_i}}{M} \quad (10)$$

$$Recall = \frac{\sum_{i=1}^{M} \frac{TP_i}{TP_i+FN_i}}{M} \quad (11)$$

$$F1-score = 2\frac{(Recall \times Precision)}{(Recall+Prevission)} \quad (12)$$

TABLE IV. ESTIMATED PERFORMANCE METRICS

	Normal	***Covid-19***	***Pneumonia***	***Average***
Accuracy(%)	95	96	94	95
Precision(%)	94	97	92	94

Where M is the total number of classes (M = 3 in our study) and i=1, 2, 3, corresponding to normal, Covid-19, and pneumonia respectively. To find the metrics for each class separately, the expressions in the numerators are used without dividing by M. The estimated metrics for the proposed method are illustrated in Table IV.

IV. DISCUSSION

Most of the resent state-of-the-art literature reported in machine learning detection of Covid-19 adopted deep learning through CNN. However, the parameters employed in the analysis of such work are huge, actually millions [17]. For example, GoogleNet-V1 about 5 million [25], ResNet-50 about 25 million [26], AlexNET about 60 million [27] and VGG-16 about 138 million parameters [28]. Consequently, the time required for training and testing is also large (in the range of thousands of seconds), even with the use of multiple graphics processing units (GPU). On the other hand, the number of parameters employed in neural network-based machine learning techniques, such as the proposed one, is in the range of thousands and the processing times are tens of seconds for both training and testing even without GPU's.

V. CONCLUSIONS

Covid-19 is a serious pandemic threatening mankind. The rapid spread of severe acute respiratory syndrome coronavirus 2 (SARS-CoV-2) has led to the COVID-19 worldwide pandemic. Developing highly accurate methods for the identification and isolation of SARS-CoV-2 infected patient is critical. Machine learning is implemented to automatically detect Covid-19 using features extracted from Chest X-ray images. This work employs features based on DCT spectral transformations of CXR images subblocks. No spatial features are incorporated. The DCT energy compaction property is employed to compress each spectral subblock. The compressed spectrum is further manipulated through averaging windows to reduce the total number of feature elements representing each CXR image. Multilayer NN is implemented to classify sets containing Covid-19, Normal and Pneumonia. The NN converged rapidly achieving very low mean squared error. The proposed method achieved an accuracy of 95 % for normal, 96% for Covid-19 and 94% for pneumonia patients. Therefore, this method is able to achieve an average accuracy of 95%. The average precision achieved is 94%. While achieving a comparable accuracy, the computational burden and the time required for both training and testing of the proposed method is very low compared to the state-of-the-art methods based on convolutional neural networks deep learning.

ACKNOWLEDGMENT

We would like to thanks following data collecting members of Dubai Health Authority - Rashid Hospital - U.A.E.:

Dr. Eman Ibrahim Elzain Hassan

Dr. Ahmed Bedair Mohamed

Dr. Khalid Alattar

Mr. Manoj Madhavan Nair Girijarajam.

REFERENCES

[1] P. Huang., "Use of Chest CT in Combination with Negative RT-PCR Assay for the 2019 Novel Coronavirus but High Clinical Suspicion", Radiology, vol. 295, no. 1, pp. 22-23, 2020.

[2] Y. Fang, H. Zhang, J. Xie, M. Lin, L. Ying, P. Pang, "Sensitivity of chest CT for COVID-19: Comparison to RT-PCR", Radiology, vol 296, no. 2, pp.115-117, 2020.

[3] W. Kong, P.P. Agarwal, "Chest imaging appearance of COVID-19 infection", Radiology: Cardiothoracic Imaging, vol. 2, no. 1,pp.1-4, 2020.

[4] D. Cozzi, M. Albanesi, E. Cavigli, C. Moroni, A. Bindi, S. Luvarà, S. Lucarini, S. Busoni, L. N. Mazzoni,V. Miele, "Chest X-ray in new coronavirus disease 2019 (COVID-19) infection: Findings and correlation with clinical outcome", La Radiologia Medica, vol. 125, no. 8, pp. 730-737, Aug. 2020.

[5] S. Ghosh, " Deep Learning Framework Integrating Spectral and Spatial Features for Image-Assisted Medical Diagnostics", IEEE Access, vol. 9, pp. 163686-163696, 2021.

[6] S.Sharma, S.Tiwari, "COVID-19 Diagnosis using X-Ray Images and Deep learning", Proceedings of the International Conference on Artificial Intelligence and Smart Systems (ICAIS-2021), pp. 344-349, 2021.

[7] L.Wang, Z. Q. Lin, and A.Wong, "COVID-Net: A tailored deep convolutional neural network design for detection of COVID-19 cases from chest X-ray images", Sci. Rep., vol. 10, no. 1, pp. 1-12, Dec. 2020, Vol. 50, No. 6, pp. 371-375, 2017.

[8] G. Jain, D. Mittal, D. Thakur, M.K. Mittal, "A deep learning approach to detect Covid-19 coronavirus with X-Ray images", Biocybern. Biomed.Eng. vol.40, no.4, pp.1391–1405, 2020.

[9] A.M. Ismael, A. Şengür, "Deep learning approaches for COVID-19 detection based on chest X-ray images", Expert Syst. Appl., vol.164, pp.1-11, 2021.

[10] A. Makris, I. Kontopoulos, K. Tserpes, "COVID-19 detection from chest X-ray images using deep learning and convolutional neural networks"medRxiv,pp.1-14, 2020.

[11] S. Asif, Y. Wenhui, H. Jin, Y. Tao, S. Jinhai, "Classification of COVID-19 from chest X-ray images using deep convolutional neural networks"medRxiv,pp.1-7, 2020.

[12] A. K. Das, S. Ghosh, S. Thunder, R. Dutta, S. Agarwal, A. Chakrabarti, "Automatic COVID-19 detection from X-ray images using ensemble learning with convolutional neural network", Pattern Analysis and Applications, pp.1111-1124, 2021.

[13] A. Ridhi, R.Kumar, V.Bansal, H.Buckchash, "AI-based Diagnosis of COVID-19 Patients Using X-ray Scans with Stochastic Ensemble of CNNs", Phys Eng Sci Med. , pp. 1-15, 2021.

[14] A. Gupta, S.G. Anjum, R. Katarya, "InstaCovNet-19: A deep learning classification model for the detection of COVID-19 patients using Chest X-ray", Appl. Soft Comput.,Vol.99, pp.1-13, 2021.

[15] E. Hussain, M. Hasan, M.A. Rahman, I. Lee, T. Tamanna, M.Z. Parvez, "CoroDet: A deep learning based classification for COVID-19 detection using chest X-ray images",Chaos Solitons Fractals, vol.142, pp. 1-12, 2021.

[16] M. Canayaz, "MH-COVIDNet: Diagnosis of COVID-19 using deep neural networks and meta-heuristic-based feature selection on X-ray images", Biomed. Signal Process. Control, vol. 64, pp.1-12, 2021.

[17] A.Z. Khuzani, M. Heidari, S.A. Shariati, "COVID-Classifier: An automated machine learning model to assist in the diagnosis of COVID-19 infection in chest x-ray images", medRxiv, pp.1-6, 2020.

[18] T. I. Haweel, "A new square wave transform based on the DCT", Signal Process, vol.81, pp. 2309–2319, 2001.

[19] K. Sayood, "Introduction to Data Compression", 2000.

[20] D. Puchala, "Approximate calculation of 8-point DCT for various scenarios of practical applications",EURASIP Journal on Image and Video Processing, pp.1-34, 2021.

[21] C. Lv, "Levenberg-Marquardt Backpropagation Training of Multilayer Neural Networks for State Estimation of A Safety Critical Cyber-Physical System", IEEE Transactions on Industrial Electronics, Vol. 14, no. 8, pp. 3436-3446, Aug 2018.

[22] X.N. Bui, "Optimizing Levenberg–Marquardt backpropagation technique in predicting factor of safety of slopes after two-dimensional OptumG2 analysis", Engineering with Computers , pp.94-952, 2020 .

[23] T. Kaur, T. K. Gandhi,B. K. Panigrahi, "Automated diagnosis of COVID-19 using deep features and parameter free BAT optimization", IEEE J. Transl. Eng. Health Med., vol. 9, pp.1-9, 2021.

[24] J.Eduardo, "Fast COVID-19 and Pneumonia Classification Using Chest X-ray Images", Mathematics, vol.8, pp.1-19, 2020.

[25] C.Szegedy,W.Liu, Y.Jia, S.Reed, "Going Deeper with Convolutions", arXiv:1409.4842, pp.1-12, 2014.

[26] K.He, X. Zhang, S. Ren, J. Sun, "Deep Residual Learning for Image Recognition", arXiv:1512.03385, pp.1-12, 2015.

[27] A. Krizhevsky, I. Sutskever, G. Hinton, " ImageNet classification with deep convolutional neural networks", Adv. Neural. Inf. Process. Syst. vol.25, pp.1097–1105 ,2012.

[28] K. Simonyan, A. Zisserman, "Very Deep Convolutional Networks for Large-Scale Image Recognition", arXiv:1409.1556 , pp.1-14, 2014.

[29] A. Shazia, "A comparative study of multiple neural network for detection of COVID-19 on chest X-ray", EURASIP Journal on Advances in Signal Processing, pp.1-16, 2021.